

Spectroscopic Characterization of the Isolated SF₆[−] and C₄F₈[−] Anions: Observation of Very Long Harmonic Progressions in Symmetric Deformation Modes upon Photodetachment

Joseph C. Bopp, Joseph R. Roscioli, and Mark A. Johnson

Sterling Chemistry Laboratory, Yale University, P.O. Box 208107, New Haven, Connecticut 06520

Thomas M. Miller[†] and A. A. Viggiano

Air Force Research Laboratory, Space Vehicles Directorate, Hanscom Air Force Base, Massachusetts 01731-3010

Stephanie M. Villano, Scott W. Wren, and W. Carl Lineberger*

JILA and Department of Chemistry, University of Colorado, Boulder, Colorado 80309

Received: October 4, 2006; In Final Form: January 10, 2007

Spectroscopic studies of the SF₆[−] and *c*-C₄F₈[−] anions are reported to provide experimental benchmarks for theoretical predictions of their structures and electron binding energies. The photoelectron spectrum of SF₆[−] is dominated by a long progression in the S–F stretching mode, with an envelope consistent with theoretical predictions that the anion preserves the *O_h* symmetry of the neutral, but has a longer S–F bond length. This main progression occurs with an unexpectedly strong contribution from a second mode, however, whose characteristic energy does not correspond to any of the neutral SF₆ fundamental vibrations in its ground electronic state. The resulting doublet pattern is evident when the bare ion is prepared with low internal energy content (i.e., using N₂ carrier gas in a free jet or liquid nitrogen-cooling in a flowing afterglow) but is much better resolved in the spectrum of the SF₆[−]·Ar complex. The infrared predissociation spectrum of SF₆[−]·Ar consists of a strong band at 683(5) cm^{−1}, which we assign to the ν₃ (t_{1u}) fundamental, the same mode that yields the strong 948 cm^{−1} infrared transition in neutral SF₆. One qualitatively interesting aspect of the SF₆[−] behavior is the simple structure of its photoelectron spectrum, which displays uncluttered, harmonic bands in an energy region where the neutral molecule contains about 2 eV of vibrational excitation. We explore this effect further in the *c*-C₄F₈[−] anion, which also presents a system that is calculated to undergo large, symmetrical distortion upon electron attachment to the neutral. The photoelectron spectrum of this species is dominated by a long, single vibrational progression, this time involving the symmetric ring-breathing mode. Like the SF₆[−] case, the *c*-C₄F₈[−] spectrum is remarkably isolated and harmonic in spite of the significant internal excitation of a relatively complex molecular framework. Both these perfluorinated anions thus share the property that the symmetrical deformation of the structural backbone upon photodetachment launches very harmonic motion in photoelectron bands that occur far above their respective adiabatic electron affinities.

I. Introduction

Both SF₆ and *c*-C₄F₈ have industrial applications as reagents in etching plasmas and insulating gases for high-voltage devices. In addition, both molecules have long lifetimes in the upper atmosphere and are considered greenhouse gases whose atmospheric lifetimes are, in part, controlled by electron attachment.¹ These two perfluorinated molecules are of fundamental interest and share the propensity to nondissociatively attach low-energy electrons, indicating that the corresponding anions have a very long lifetime with respect to autodetachment.^{2,3} One of the reasons for this slow autodetachment undoubtedly results from the change in structure of the molecular framework upon anion formation. For these reasons, both molecules have been the subject of many studies that have focused on the characterization of the neutral and the formation and reactivity of the anion;^{4–10}

however, very few spectroscopic studies have addressed the structural aspects of the ions.

Of particular interest, SF₆ has been the focus of intense study for the past 30 years.^{11–22} The neutral structure has been well characterized by several Raman and infrared studies,²³ and only two reports address the structural aspects of the ion through spectroscopy.^{24,25} An early study commented only on the lack of observed photodetachment in the near-ultraviolet,²⁴ far above the adiabatic threshold, whereas a matrix isolation study identified a single weak vibrational transition near 600 cm^{−1}.²⁵ More recently, computational results predict that the *O_h* symmetry of SF₆ is retained upon attachment of an electron; however, the S–F bonds are elongated by about 0.2 Å.²⁶

As with SF₆, there is a large geometry change upon attachment of an electron to *c*-C₄F₈. It is known from spectroscopic studies that the geometry of the neutral is bent (*D_{2d}* symmetry) and several vibrational frequencies have been measured.^{27–33} Far less is known about the anion structure.

[†] Also, Institute for Scientific Research, Boston College.

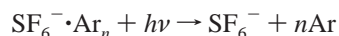
Recent ESR studies have shown that the anion structure is planar with D_{4h} symmetry³⁴ and computational results predict that the added electron is delocalized in a “p-like” orbital extending over the entire molecule, strengthening the four C–C bonds via π -bonding interactions, and weakening the eight C–F bonds via σ^* -antibonding interactions.^{34,35}

The present study investigates what happens when an electron is attached to the closed shell perfluorinated molecules SF₆ and *c*-C₄F₈. We present the photodetachment and infrared spectra of the cooled, isolated SF₆ anion. Internal energy control was effected using both Ar-tagging in a free jet ion source and liquid nitrogen cooling in a relatively high-pressure (~0.5 Torr) flowing afterglow ion source. We also report the photoelectron spectrum of the *c*-C₄F₈ anion, and then discuss the similar characters of the two species.

II. Experimental Section

Pulsed laser photoelectron and infrared predissociation spectroscopies of SF₆⁻ were carried out using the Yale double focusing tandem time-of-flight spectrometer, described previously.³⁶ The SF₆⁻·Ar_{*n*} clusters were created by entraining³⁷ SF₆ into a pulsed supersonic expansion of pure Ar, ionized with a 1 keV electron beam counterpropagated along the axis of the free jet. Photoelectron spectra were collected using the second and third harmonics from a Spectra-Physics DCR-2 Nd:YAG laser. The laser polarization was oriented along the axis of the field-free time-of-flight photoelectron spectrometer,³⁸ which has its drift axis perpendicular to the molecular beam direction. Reported spectra are the sum of approximately 100–300k laser shots.

Infrared predissociation spectra were collected using the argon “messenger atom” technique:³⁹



Laser excitation in the energy range 600–800 cm⁻¹ was achieved using a Nd:YAG pumped OPO/OPA (LaserVision) in which the final parametric conversion is executed in AgGaSe₂ to give an output energy of about 30 μ J/pulse at 650 cm⁻¹ (where the features occur in SF₆⁻). Reported spectra are an accumulation of approximately 25 individual scans, which are corrected for laser energy variations over the scan range.

Photoelectron spectra were also obtained using a flowing afterglow photoelectron spectrometer at JILA.⁴⁰ In this instrument, ions are created in a flowing afterglow source, mass selected and crossed with the 351 nm line of a cw Ar-ion laser in an external buildup cavity. Electrons ejected into a very small solid angle perpendicular to the ion-laser interaction region pass through a hemispherical analyzer and are imaged onto a position sensitive detector. Angular distribution measurements can be made by rotating the laser polarization with a half wave plate. One of the benefits of this instrument is that ions are created under well-characterized thermal conditions controlled by the buffer gas temperature. Cooling the internal energy of the ions is clearly of paramount interest in the determination of the anion equilibrium structures. With this source, the anions are relaxed to room temperature by multiple collisions with He carrier gas (~0.5 Torr, 3–10 ms resonance time)⁴¹ and can be further cooled by surrounding the flow tube with a liquid nitrogen jacket. Prior experience with this arrangement suggests that the resulting ions are prepared in the 150–200 K range.⁴²

III. Results and Discussion

III.A. SF₆⁻ Photoelectron Spectra. III.A.1. Bare Molecule: Overview and Ion Source Dependence of the Photoelectron

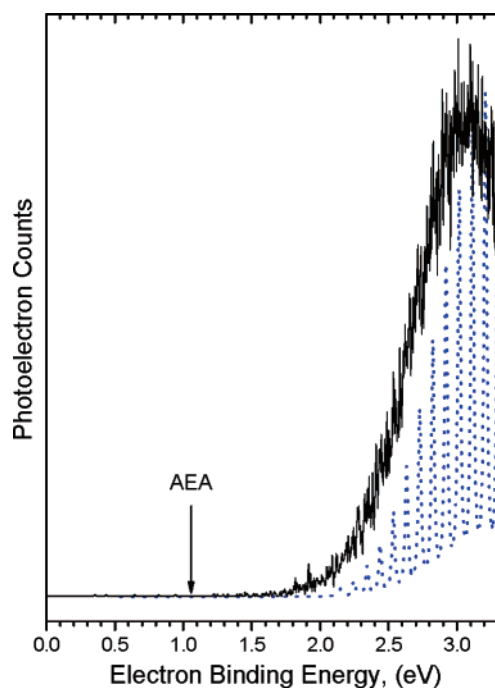


Figure 1. Photoelectron spectrum of the bare SF₆⁻ anion from the pulsed ion source tuned to maximize ion signal. The arrow indicates the adiabatic electron affinity (AEA) from ref 43. The dotted line indicates the expected vibrational pattern for the calculated (O_h) anion structure from ref 26 including only the ν_1 , S–F symmetric stretching vibration.

Spectrum. Figure 1 presents the photoelectron spectrum of the bare SF₆⁻ ion obtained with the pulsed source tuned to maximize parent ion intensity (e.g., large partial pressure of SF₆, low backing pressure). The most striking aspect of this spectrum is that, in spite of the fact that the adiabatic electron affinity (AEA) arrow in Figure 1) is reported to lie in the 1 eV range,⁴³ significant photoelectron activity does not begin until almost 2 eV. The 3 eV location of the band maximum (vertical electron detachment energy, VDE) is qualitatively consistent, however, with calculations (CCSD(T)/6-311+G(2df)) of the anion structure,²⁶ as summarized by the calculated potential energy curves presented in Figure 2. The global minimum for the SF₆⁻ anion is calculated to have considerably elongated S–F bonds (by ~0.2 Å), but to retain the O_h symmetry of the neutral. The curves in Figure 2 describe the (harmonic) potential energy variation along the S–F symmetric stretching (ν_1) normal coordinate, which is the reaction coordinate that mediates the structural transformation between the neutral and anion geometries. Note that the zero-point vibrational wavefunction of the anion (inset in lower curve in Figure 2) provides essentially no vibrational overlap at the band origin. More quantitatively, the inset in Figure 1 (dotted line) presents the vibrational distribution expected for a one-dimensional Franck–Condon analysis at the harmonic level using the curves in Figure 2, which clearly explains the general character of the observed broad feature.

Because the vertical detachment process leads to such large internal energy content in neutral SF₆, it is perhaps not surprising that the spectrum (Figure 1) does not display resolved vibrational fine structure. This is especially relevant in the case of SF₆ where extensive theoretical effort has addressed its behavior in this “quasi-continuum” spectral regime in the context of infrared multiphoton dissociation. Of course, heterogeneous broadening arising from vibrational hot bands could also act to obscure distinct band progressions, and we therefore attempted to cool the ion by tuning the pulsed jet source conditions (high backing

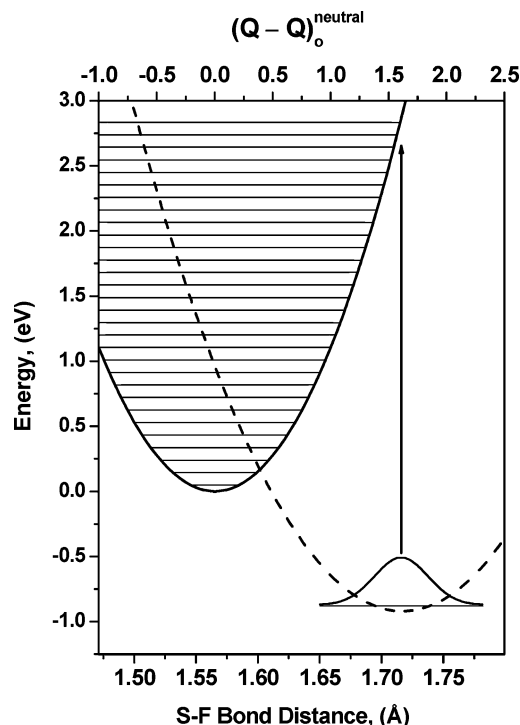


Figure 2. Harmonic potential curves for the ν_1 , S–F symmetric stretching normal mode displacement in SF_6 (solid line) and SF_6^- (dashed line). The zero-point vibrational wavefunction is also included for the anion to illustrate the expected range of vibrational overlap with the neutral curve. The arrow indicates the expected vertical detachment energy in the harmonic limit (~ 2.8 eV). All information used for these potentials was taken from ref 26.

pressure, low partial pressure of SF_6), and by generating it in a flowing afterglow ion source that yields many more collisions with buffer gas than are available using the free jets.

Expanded views of two representative spectra are presented in Figure 3. The upper spectrum was obtained using the Yale pulsed instrument, where SF_6^- was generated by entraining trace SF_6 in an expansion of N_2 at a stagnation pressure of 5 atm. In the lower spectrum, SF_6^- was prepared in a liquid nitrogen-cooled flowing afterglow source at JILA employing He as a carrier gas. Most importantly, discernible vibrational fine structure appears in both cases with similar depths of modulation and location of the maxima, thus reflecting a robust property of the ion that is independent of the method of preparation.

Although the overall envelope of the photoelectron spectrum is in line with expectations, careful inspection of the spectra in Figure 3 indicates that though there are indeed prominent peaks spaced by ν_1 (solid lines), there is an additional progression appearing as interlopers in the ν_1 series (dotted lines). Note that these features appear much broader than the 7 meV resolution of the JILA spectrometer, and one can question whether residual vibrational hot bands are still at play in the better resolved spectrum arising from the cooler ions. Experience with the flowing afterglow source suggests that the ions are likely to occur in the 150–200 K temperature range,⁴² and the calculated SF_6^- frequencies vary from 237 to 772 cm^{-1} , as indicated in Table 1.²⁶ This would imply that there is plausible excitation of ν_4 (306 cm^{-1}), ν_5 (336 cm^{-1}), and ν_6 (237 cm^{-1})²³ in the thermal ensemble. Of these, the ν_4 mode could explain the interloper as a hot band occurring about 300 cm^{-1} below the members of the main progression. It would seem fortuitous, however, that the extent of internal excitation would be almost exactly the same in the jet and afterglow sources, as these yield almost identical spectra. To help clarify the situation, we

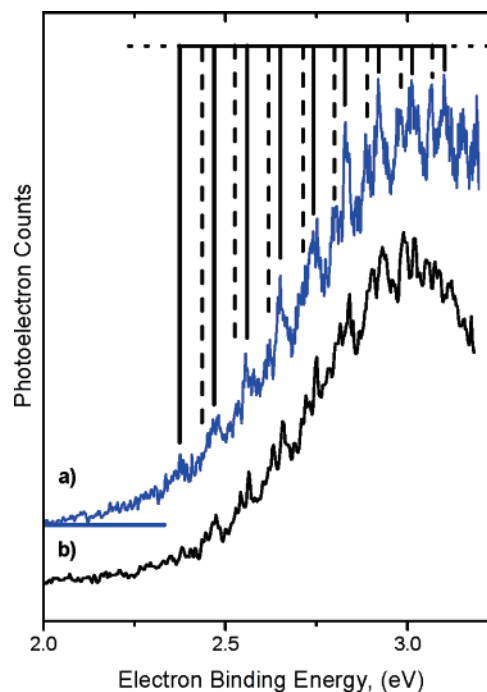


Figure 3. Comparison of bare SF_6^- photoelectron spectra (a) from the pulsed Yale source with nitrogen being used as the carrier gas, and (b) from the JILA spectrometer in which liquid nitrogen was used to cool the (He) flowing afterglow ion source. We highlight the more pronounced progression arising from the excitation of the ν_1 mode in the neutral with the solid line, whereas the dashed line indicates a second progression that appears with the same characteristic spacing.

TABLE 1: Theoretical Frequencies (cm^{-1}) Calculated at the MBPT(2) Level of Theory for Both SF_6 and SF_6^- along with the Experimental Frequencies for SF_6 .

vibrational mode	SF_6		SF_6^- theory ²⁶
	theory ²⁶	expt. ²³	
ν_6 (t_{2u})	346	348	237
ν_5 (t_{2g})	519	524	336
ν_4 (t_{1u})	611	615	306
ν_2 (e_g)	655	643	447
ν_1 (a_{1g})	779	775	626
ν_3 (t_{1u})	965	948	722

therefore turned to argon-tagging as a means to limit the internal energy content of the molecular anion, with the results summarized in the next section.

III.A.2. Argon Tagged Photoelectron Spectra. Photoelectron spectra (3.5 eV) of the $\text{SF}_6^- \cdot \text{Ar}_n$, $n = 0-2$, clusters are compared in Figure 4. The spectrum with a single Ar atom (Figure 4b) displays significantly sharper peaks than either of those obtained for the bare molecule (Figure 3), and the pattern appears *uniformly* shifted by about 52 meV toward higher binding energy. Most importantly, the tagged spectrum clearly displays the second series of interloper peaks, with peak intensities similar to those evident in the bare ion spectra. The Ar atom therefore does not appear to perturb the structure, but more likely it further quenches the SF_6^- subsystem into its ground vibrational state. Interestingly, addition of a second Ar atom again shifts the spectrum toward higher binding energy (this time by 28 meV), but the peaks become *less* well resolved than in the $n = 1$ case. Even with this broadening, however, the series of two peaks can be readily discerned, and it is likely that the broadening caused by the second Ar results from the distribution of Ar isomers available according to the relative locations of the two Ar atoms.^{44,45}

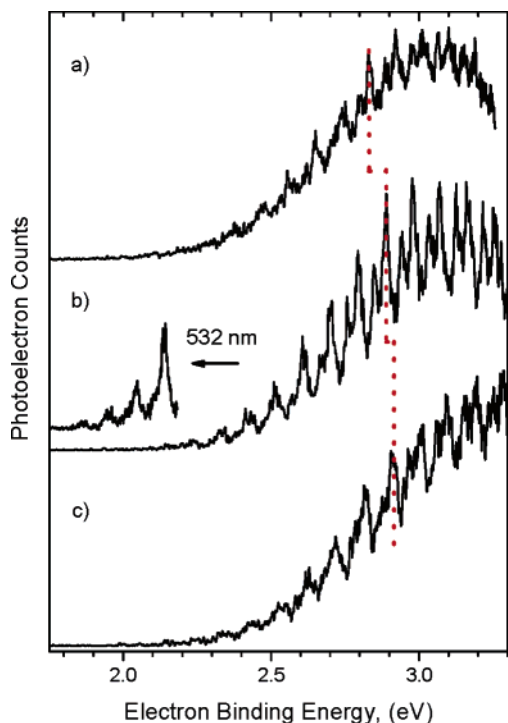


Figure 4. Photoelectron spectra (3.495 eV) of the SF₆⁻·Ar_n complexes (a) bare SF₆⁻ reproduced from Figure 3a, (b) SF₆⁻·Ar, and (c) SF₆⁻·Ar₂. The dotted line highlights the evolution of a particular vibrational feature to indicate the solvent shifts. The inset spectrum in (b) was taken at 2.33 eV photoexcitation to follow the vibrational progression to lower levels.

The considerations discussed in section III.A.1 suggest that these vibrational progressions occur very far above the photo-detachment threshold, which implies that the vibrational levels in the binding energy region below 2.1 eV are suppressed by poor vibrational overlap. One way to experimentally access this Franck–Condon “forbidden” region is to carry out the photo-detachment with a very powerful laser operating at a lower photon energy. Such a requirement is easily satisfied by use of the Nd:YAG second harmonic beam (2.33 vs 3.495 eV), with the resulting spectrum of the *n* = 1 complex displayed as an inset in Figure 4b. Vibrational peaks are indeed recovered in this configuration, which extends the progression to at least four lower vibrational levels than were apparent when 3.495 eV excitation was used.

The emergence of new peaks upon 2.33 eV excitation establishes that the intensity of the spectrum is very weak until well above the AEA, making it impossible to extract this important thermodynamic quantity from a cursory analysis of the spectral envelope. In this context, it is important to emphasize that, although thermochemical determinations indicate that the spectrum begins at around *v* = 10, the progression that emerges after this delayed onset is quite harmonic. The relative simplicity of the spectrum is surprising in a seven-atom molecule that contains, at the maximum of the vibrational progression, about 2 eV of internal energy or roughly 50% of the bond energy! The simplicity of the photoelectron spectra indicates that excitation of the symmetric stretching vibration can survive for many vibrational periods before the energy is dissipated into the remaining modes.

III.A.3. Vibrational Analysis of the Photoelectron Spectrum.

We focus on the SF₆⁻·Ar case (Figure 4b) because it best articulates the two-mode pattern evident in the spectrum of the bare molecule (Figure 3). First, we note that the main progression is remarkably harmonic at our resolution with a constant

spacing of 749(19) cm⁻¹, which is clearly assigned (as expected) to the 775 cm⁻¹ symmetric S–F stretching mode (*ν*₁) in neutral SF₆. Note that at lower levels of vibrational excitation accessible by direct absorption from the ground state neutral, high-resolution spectroscopic analysis indicates that this mode indeed exhibits only rather small coupling constants in the anharmonic Hamiltonian. Inspection of the calculated spectrum involving only this mode (Figure 1) suggests that the peak of the vibrational progression occurs at about *v* = 27. This is consistent with the slightly smaller (by 26 cm⁻¹) observed spacing relative to the fundamental transition because *X*₁₁ = -0.896 cm⁻¹.⁴⁶

Assignment of the second active mode in the spectrum is much less obvious. First, the interloper spacing remains constant throughout the spectrum, so that we can rule out a situation where two different modes are independently involved in Gaussian-like progressions starting from the same initial state of the anion. As mentioned above, the consistency of the spectra in different ion sources (including Ar tagging) indicates that the second mode does not derive from a hot-band arising from excited vibrational levels of the ground electronic state. In addition, its assignment to a combination band involving excitation of *ν*₁ with one quantum from a second mode in the neutral is not consistent with the observed splittings. Specifically, the second mode is systematically displaced by about 440(10) cm⁻¹ relative to the main features, which does *not* correspond to any of the fundamental frequencies at play in neutral SF₆. The modes that are the closest frequencies are *ν*₅ (*t*_{2g} symmetry) at 348 cm⁻¹ and *ν*₆ (*t*_{2u} symmetry) at 524 cm⁻¹.²³ One may suspect that anharmonic coupling with very high levels of *ν*₁ could reduce the effective quantum somewhat, but recall that the displacement of the secondary peak is constant (within the experimental resolution) over the spectrum. This indicates that anharmonicity is not significant, and the energy mismatch thus rules out a combination band assignment based on one quantum of another vibrational mode.

Having argued against assignment of the additional peaks to either vibrational hot bands or to combination bands involving 0 → 1 transitions of another mode, we next entertain the possibility that higher harmonics play a role in the combination band scenario. In this context, the closest match to the observed splitting is provided by 2*ν*₄ (~1200 cm⁻¹). Note that this is a nontotally symmetric, IR active mode and therefore we would not expect odd quanta to be populated in photodetachment. It is not obvious, however, why such an overtone would be so intense. For example, the expected Franck–Condon factors for 0 → 2 transitions that arise from the large (factor of ~2; see Table 1) change in the frequency of this vibration upon photodetachment are only about 5% of those calculated for the Δ*v* = 0 transitions. Thus, it is likely that some displacement of this mode would be required to achieve the large intensities of the putative overtones, which would, in turn, suggest that the anion geometry might conform to C_{4v} rather than O_h symmetry.

Although we note that past reports have indeed suggested that SF₆⁻ adopts this distorted C_{4v} geometry in the ground state,^{24,47} most recent calculations find a robust minimum with O_h symmetry.^{26,48} This casts doubt on the overtone/combination band hypothesis for the doublet pattern in the photoelectron spectrum outlined above. As an alternative scenario, we point out that the observed behavior is quite consistent with what one would expect if the anion is formed with population in a low-lying, electronically excited state with nearly the same geometry as the ground state. Although *ab initio* calculations do not predict such an additional electronic state,⁴⁸ it is possible that the open shell nature of the radical anion could support a very low-lying

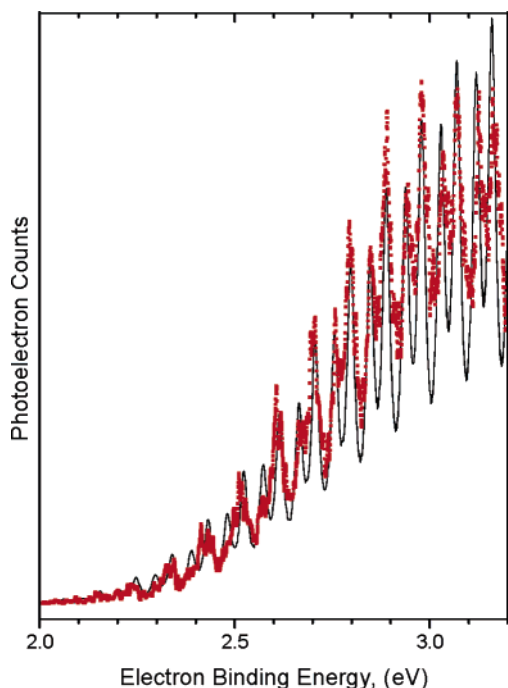


Figure 5. Expanded view of the $\text{SF}_6^- \cdot \text{Ar}$ photoelectron spectrum (3.495 eV), along with a simulated spectrum (solid line) corresponding to the superposition of two separate Gaussian distributions shifted relative to each other by $440(10) \text{ cm}^{-1}$.

state within the same electronic configuration. For example, depending on the precise nature of the SOMO that accommodates the excess electron, an excited state based on the spin-orbit interaction would have a geometry very similar to that of the ground state, and the population in this state would be very difficult to relax.^{49–54} This scenario nicely explains the shape of the photoelectron spectrum, as it would yield two Gaussian-like vibrational progressions terminating on ν_1 levels of the neutral, with envelopes displaced from one another by the electronic splitting in the anion.

Figure 5 presents a fit of the $\text{SF}_6^- \cdot \text{Ar}$ photoelectron spectrum to two such overlapping, bell shaped progressions, which accurately recover the observed behavior with a displacement of $440(10) \text{ cm}^{-1}$. It is interesting that this value is, perhaps fortuitously, quite close to the spin-orbit splitting displayed by the isolated S^- anion.⁵⁵

The identification of the correct molecular physics that underlies the extra progression in the photoelectron spectrum is a clear target for further theoretical work on this important anion. In particular, it would be useful to evaluate the expected magnitude of the spin doubling present in the ${}^2\text{A}_{1g}$ anionic ground state, as well as the shape of its potential surface along deformations that would carry the system toward C_{4v} symmetry. One aspect of this problem that has not been addressed, for example, is the possible role of vibronic interactions with low-lying electronically excited configurations.

III.B. Vibrational Predissociation Spectroscopy of $\text{SF}_6^- \cdot \text{Ar}_n$

The discussion of the unexpected vibrational activity in the photoelectron spectrum naturally raised questions about the actual geometry of the anion and validity of the harmonic approximation to describe the vibrational motion on the ground state surface. Although most S–F fundamentals are calculated to occur at very low energy, the ν_3 mode, which is the analogue of the strong 948 cm^{-1} transition in neutral SF_6 ,²³ is anticipated to occur at 722 cm^{-1} ,²⁶ which is just accessible using parametric conversion in AgGaSe_2 . Figure 6 presents the predissociation spectra of $\text{SF}_6^- \cdot \text{Ar}_n$, $n = 1$ (Figure 6b) and $n = 2$ (Figure 6a),

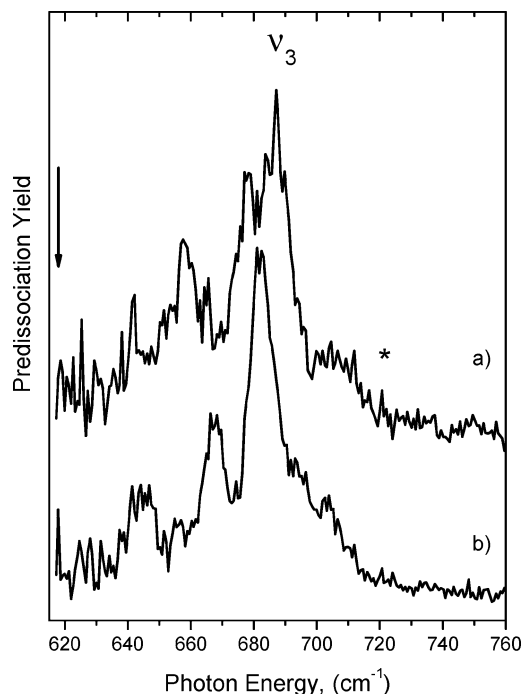


Figure 6. Vibrational predissociation spectra of the ν_3 band for (a) $\text{SF}_6^- \cdot \text{Ar}_2$ and (b) $\text{SF}_6^- \cdot \text{Ar}$. The arrow indicates the position of the ν_3 band recovered for SF_6^- by Jacox, in a Ne matrix.²⁵ The asterisk indicates the harmonic ν_3 transition energy calculated by Gutsev and Bartlett.²⁶

with the predicted (harmonic) location of the ν_3 mode indicated by an asterisk.²⁶ On the basis of this agreement, we assign the feature at $683(5) \text{ cm}^{-1}$ to the ν_3 fundamental in the Ar-solvated species. It is useful to mention that the analogous transition in an Ar matrix has been reported by Jacox²⁵ (denoted by an arrow in Figure 6) who assigned an isolated, relatively sharp band at 619 cm^{-1} to this transition in a study where photodepletion was used to identify the features arising from anionic species.

The most important observation is that the main band at 683 cm^{-1} is not significantly perturbed by the addition of the second Ar atom, where the main effect is to broaden the feature. There is, however, clearly resolved fine structure in the $n = 1$ spectrum that is slightly changed in that of $n = 2$. The most pronounced side bands appear on the low-energy side and are thus not likely due to excitation of $\text{SF}_6^- \cdot \text{Ar}$ soft modes, but rather to internal excitations in SF_6^- . We note that a minor perturbation by the Ar atom is anticipated from the behavior of the photoelectron spectra (Figure 4), where not only were the spectra solvent-shifted to higher energy, but the doublet nature of the progressions was somewhat washed out in the $n = 2$ spectrum relative to that displayed by $n = 1$. In the case of the vibrational band, it is useful to mention that this vibration is triply degenerate in the isolated molecule (if it indeed has O_h symmetry) and thus some splitting is expected as Ar attachment breaks the symmetry of the species, presumably into two peaks if the Ar is localized on one F atom. There are more than three distinct components in the $n = 1$ spectrum, however, precluding a trivial assignment to such a lifted degeneracy scenario. Like the situation encountered in the Ar-dependent photoelectron spectra, it is expected that the second Ar will yield a more complex vibrational predissociation spectrum according to the number of isomers available for the second binding site. This rationalizes the broadening evident in the $n = 2$ vibrational spectrum. It would clearly be of value at this point to acquire the spectrum of either the cold bare ion or to obtain a predissociation spectrum using a more weakly binding messenger. We attempted a study

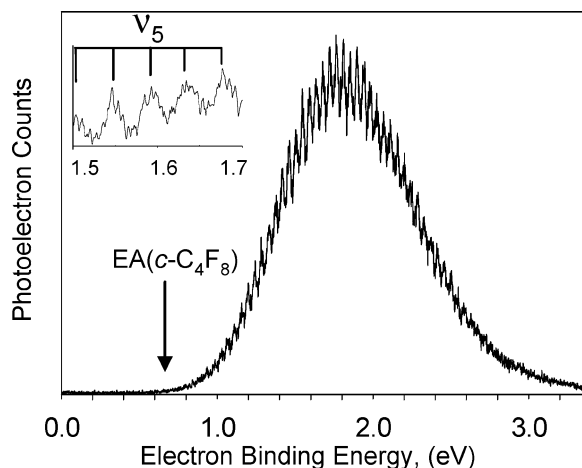


Figure 7. The 351 nm photodetachment spectrum of *c*-C₄F₈⁻ taken at the magic angle using a flowing afterglow photoelectron spectrometer. A regular harmonic progression is present with spacing corresponding to the ν_5 frequency of 355(3) cm⁻¹. The EA(*c*-C₄F₈) determined by Miller⁹ is indicated by a vertical arrow.

using Ne but were not successful in synthesizing the necessary parent ions. Our primary conclusion from the vibrational spectra is that the harmonic expectation for an *O_h* symmetry ion is largely in agreement with the observed band position.

III.C. Photoelectron Spectrum of C₄F₈⁻. The observation of regular vibrational motion at very high levels of excitation in the ground electronic state following electron photodetachment from SF₆⁻ is rather unusual for such a large system. We therefore take this opportunity to highlight a related case that we have encountered involving *c*-C₄F₈⁻ photodetachment. Figure 7 shows the 351 nm photoelectron spectrum of *c*-C₄F₈⁻ obtained using a flowing afterglow photoelectron spectrometer. In this instrument, ions have a room-temperature vibrational and rotational distribution from collisions with He buffer gas (~0.5 Torr, 3–10 ms resonance time) prior to leaving the source region.⁴¹ Like the SF₆⁻ spectrum, an extremely long and harmonic progression is observed that extends almost 2 eV (approximately 42 quanta) into the vibrational manifold of the ground electronic state of *c*-C₄F₈!

Flowing afterglow Langmuir probe studies find EA(*c*-C₄F₈) to be 0.63(0.05) eV⁹ (indicated by the arrow in Figure 7); two other values have also been reported.^{11,56} As elaborated later, we believe this flowing afterglow determination to be the most reliable measurement of EA(*c*-C₄F₈). This experimental value is also in excellent agreement with a MP2/6-311G(dps) calculation by Gallup, which gave a value of 0.64 eV.³⁵ Placing the EA at 0.63(0.05) eV means that the first vibrational peak seen in the spectrum corresponds approximately to $\nu = 7$ in some mode; resolved structure is still apparent up to $\nu \sim 50$. The maximum intensity (VDE) occurs at $\nu \sim 27$, consistent with a large geometry change from anion to neutral. It is known from electron diffraction and infrared studies that the carbon framework of the neutral is bent with *D*_{2d} symmetry,^{27–33} whereas recent ESR studies have shown that anion framework is planar with *D*_{4h} symmetry.³⁴ Calculated structures (B3LYP/6-31+G(3df)) of the neutral and the anion are displayed in Figure 8. Detachment of an electron elongates the C–C bonds, shortens the C–F bonds, and increases the nonbonded F–F distance. This increase in symmetry has been predicted by computations that also show that the negative charge in the anion is a “p-like” orbital that is delocalized over the entire molecule.^{34,35} This deformation corresponds to the ν_5 mode, calculated to be 359 cm⁻¹ at the B3LYP/6-31+G(3df) level of theory. Thus,

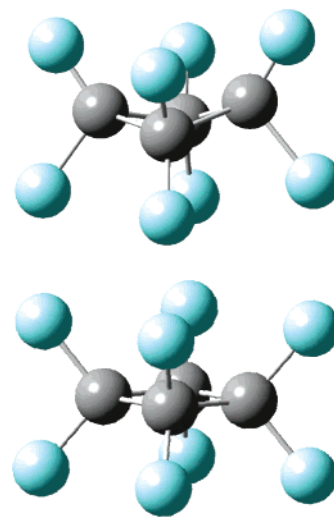


Figure 8. Calculated structures (B3LYP/6-31+G(3df)) of *c*-C₄F₈ neutral (top) and anion (bottom). The neutral structure is bent out of the plane by 8°; however, the figure is exaggerated for clarity.

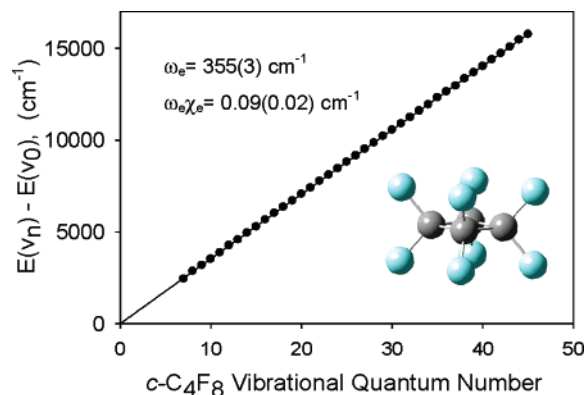


Figure 9. $[E(v_n) - E(v_0)]$ as a function of *c*-C₄F₈ vibrational quanta obtained using spacings from the spectrum in Figure 8. The solid line is the corresponding fit to these data.

we expect this mode to be active in the photoelectron spectrum, and the long progression appears to correspond to excitation of this mode.

On the basis of the size of the molecule and the large geometry change between the anion and neutral, one might expect to see an extended Franck–Condon profile with virtually no resolved features. However, what is so striking is that the spectrum is rather “diatomic-like” and remains harmonic across the entire spectrum. Although the spectrum looks like a simple progression, the peak spacing is broader than the instrument resolution of 7 meV. It is probable that there are contributions from low-frequency modes over the ν_5 progression; one likely candidate could be the ν_6 totally symmetric ring bending mode. Figure 9 shows a plot of $E(v_n) - E(v_0)$ as a function of vibrational quanta. The fact that this plot remains linear, even at high vibrational quanta, indicates that anharmonicity is small. From this plot we determine the fundamental frequency, ω_e , to be 355(3) cm⁻¹ and the first order anharmonicity, $\omega_e x_e$, to be 0.09(0.02) cm⁻¹. The long progression involves the ν_5 (A₁ symmetry) ring-breathing mode; this deformation corresponds to the reaction coordinate for the transformation from the neutral to the anion. The measured frequency is in remarkable agreement with the calculated value above and greatly improves upon the earlier 360(60) cm⁻¹ measurement reported by Mao et al.²⁹ As was pointed out with the SF₆⁻ spectrum, this long, harmonic behavior is quite unusual and indicates that there is weak

coupling from ν_5 to the rather large density of background states available at such high levels of vibrational excitation.

As previously mentioned, other EA values have been reported in the literature.^{11,56} Although the photoelectron spectrum of $c\text{-C}_4\text{F}_8^-$ does not give a direct determination of this value, it does provide an upper bound of ~ 0.75 eV. Hiraoka and co-workers measured EA($c\text{-C}_4\text{F}_8$) relative to that of SF_6 , using a pulsed electron beam high-pressure mass spectrometer.⁵⁶ They reported a value of 1.05 eV, incompatible with the photoelectron spectrum reported here. Hiraoka interpreted his observations to suggest the presence of an excited $c\text{-C}_4\text{F}_8^-$ isomer which would form at elevated temperatures (above 350 K) and undergo electron detachment. The EA of this other isomer was reported to be 0.5 eV, based upon electron-transfer equilibrium with O_2 . The single vibrational mode character of the spectrum in Figure 7 would appear to rule out the coexistence of two isomers in our spectrum. In addition, photoelectron angular distribution measurements give a smooth, minor progression of the anisotropy parameter, β , across the spectrum, inconsistent with the coexistence of a second isomer in our spectrum. Thus, though our data do not provide a definitive EA determination, they do allow a definitive choice between the two most reliable prior determinations. Thus we conclude that an EA($c\text{-C}_4\text{F}_8$) of 0.63 eV⁹ is both consistent with our data, and the most reliable value available. A detailed discussion of all of the earlier determinations of EA($c\text{-C}_4\text{F}_8$) has been recently given by Miller et al.⁹

IV. Conclusion

The photoelectron spectra of SF_6^- and $c\text{-C}_4\text{F}_8^-$ both display a strikingly extended harmonic progression that is simpler than expected. In both cases the vibrational progression is due to a breathing motion that arises from detachment of an electron that is delocalized over the entire molecule. There is also no observable signal near the measured AEA, which is consistent with a large change in geometry between anion and neutral. Despite the high levels of excitation in the neutral molecule, these motions appear relatively isolated and quite harmonic, even when the molecule contains about half of the energy required for dissociation. The vibrational bands in the Ar-tagged SF_6^- spectrum were observed to sharpen significantly relative to those obtained with a flowing afterglow ion source operating in the 150–200 K range. Although we did not carry out measurements on $c\text{-C}_4\text{F}_8^-$ with Ar tagging, the bands obtained from the flow tube preparation were narrower than those obtained for SF_6^- , suggesting that the latter is more sensitive to hot band contributions.

The active vibrational mode in SF_6 is traced to excitation of the symmetrical S–F (ν_1) vibrational mode, as expected from an O_h symmetry anion with an S–F bond length extended by about 0.2 Å from that of the neutral. This series is evident when the ion is cooled, either through pulsed supersonic expansion with N_2 , or through use of a liquid N_2 cooled flowing afterglow ion source. This primary vibrational progression is accompanied by an unexpected second vibration, which increases in intensity with increasing quanta of ν_1 . This doublet pattern is much better resolved in the spectrum of the $\text{SF}_6^- \cdot \text{Ar}$ complex, and its origin is presently unclear. One possibility is that it involves a very low-energy SF_6^- electronically excited state, possibly arising from the open shell electronic structure of the radical anion. The vibrational spectrum of the Ar complex was also obtained, which yields only one band with multiplet fine structure centered at about 683(5) cm^{-1} . This feature is assigned to the ν_3 (t_{1u}) vibrational fundamental based on harmonic calculations at the O_h minimum in the potential surface.

The only resolved vibration following electron photodetachment from $c\text{-C}_4\text{F}_8^-$ is the symmetrical ring-breathing (ν_5) mode, where the C–C bonds are slightly shortened, the C–F bonds lengthened and the F–C–F angle extended. This motion represents the reaction coordinate for the transformation between the anion and the neutral, where the anion is planar and the neutral is bent. This vibrational progression remains structured and harmonic throughout the spectrum, extending over 40 quanta into the $c\text{-C}_4\text{F}_8$ vibrational manifold.

Acknowledgment. We thank Jeffrey Headrick for valuable technical assistance in acquiring both the photoelectron and vibrational predissociation data. We also benefited from valuable discussions with Profs. K. H. Bowen and R. N. Compton, especially regarding the value of N_2 cooling in free jets. M.A.J. and W.C.L. thank the Air Force Office of Scientific Research for support of this work under grants FA-9550-06-1-00049 and FA-9550-06-1-006. A.A.V. and T.M.M. are supported by the United States Air Force of Scientific Research (AFOSR) under Project No. 2303EP4. T.M.M. is supported under contract No. FA8718-04-C-0006 to Boston College.

References and Notes

- (1) Morris, R. A.; Miller, T. M.; Viggiano, A. A.; Paulson, J. F.; Solomon, S.; Reid, G. J. *Geophys. Res., [Atmos.]* **1995**, *100*, 1287–94.
- (2) Compton, R. N.; Christophorou, L. G.; Hurst, G. S.; Reinhardt, P. W. *J. Chem. Phys.* **1966**, *45*, 4634–39.
- (3) Compton, R. N.; Hurst, G. S.; Christophorou, L. G.; Reinhardt, P. W. "ORNL-TM-1409," 1966.
- (4) Dehmer, J. L.; Siegel, J.; Dill, D. J. *J. Chem. Phys.* **1978**, *69*, 5205–6.
- (5) Field, D.; Jones, N. C.; Ziesel, J. P. *Phys. Rev. A* **2004**, *69*, 057216 (11 pages).
- (6) Ferch, J.; Raith, W.; Schroder, K. *J. Phys. B: At., Mol. Opt. Phys.* **1982**, *15*, L175–L8.
- (7) Christophorou, L. G.; Olthoff, J. K. *J. Phys. Chem. Ref. Data* **2000**, *29*, 267–330.
- (8) Christophorou, L. G.; Olthoff, J. K. *J. Phys. Chem. Ref. Data* **2001**, *30*, 449–73.
- (9) Miller, T. M.; Friedman, J. F.; Viggiano, A. A. *J. Chem. Phys.* **2004**, *120*, 7024–8.
- (10) Braun, M.; Gruber, F.; Ruf, M.-W.; Kumar, S. V. K.; Illenberger, E.; Hotop, H. *J. Chem. Phys.* **2006**, *329*, 148–62.
- (11) Lifshitz, C.; Tiernan, T. O.; Hughes, B. M. *J. Chem. Phys.* **1973**, *59*, 3182–92.
- (12) Compton, R. N.; Reinhardt, P. W.; Cooper, C. D. *J. Chem. Phys.* **1978**, *68*, 2023–36.
- (13) Babcock, L. M.; Streit, G. E. *J. Chem. Phys.* **1981**, *74*, 5700–6.
- (14) Hay, P. J. *J. Chem. Phys.* **1982**, *76*, 502–4.
- (15) Streit, G. E. *J. Phys. Chem.* **1982**, *86*, 2321–4.
- (16) Christophorou, L. G. *Electron-Molecule interactions and their applications*; Academic: New York, 1984.
- (17) Klobukowski, M.; Barandiaran, Z.; Seijo, L.; Huzinaga, S. *J. Chem. Phys.* **1987**, *86*, 1637–8.
- (18) Mock, R. S.; Grimsrud, E. P. *Chem. Phys. Lett.* **1991**, *184*, 99–101.
- (19) Datskos, P. G.; Carter, J. G.; Christophorou, L. G. *Chem. Phys. Lett.* **1995**, *239*, 38–43.
- (20) Gianturco, F. A.; Lucchese, R. R. *J. Chem. Phys.* **2001**, *114*, 3429–39.
- (21) Tachikawa, H. *J. Phys. B: At., Mol. Opt. Phys.* **2002**, *35*, 55–60.
- (22) Braun, M.; Ruf, M. W.; Hotop, H.; Allan, M. *Chem. Phys. Lett.* **2006**, *419*, 517–22.
- (23) McDowell, R. S.; Krohn, B. J.; Flicker, H.; Vasquez, M. C. *Spectrochim. Acta, Part A* **1986**, *42*, 351–69.
- (24) Drzaic, P. S.; Brauman, J. I. *J. Am. Chem. Soc.* **1982**, *104*, 13–9.
- (25) Lugez, C. L.; Jacox, M. E.; King, R. A.; Schaefer, H. F. *J. Chem. Phys.* **1998**, *108*, 9639–50.
- (26) Gutsev, G. L.; Bartlett, R. J. *Mol. Phys.* **1998**, *94*, 121–5.
- (27) Fischer, G.; Purchase, R. L.; Smith, D. M. *J. Mol. Struct.* **1997**, *405*, 159–67.
- (28) Bauman, R. P.; Bulkin, B. J. *J. Chem. Phys.* **1966**, *45*, 496–8.
- (29) Mao, C.; Nie, C. S.; Zhu, Z. Y. *Spectrochim. Acta, Part A* **1988**, *44*, 1093–8.
- (30) Beagley, B.; Calladine, R.; Pritchard, R. G.; Taylor, S. F. *J. Mol. Struct.* **1987**, *158*, 309–14.

- (31) Chang, C. H.; Porter, R. F.; Bauer, S. H. *J. Mol. Struct.* **1971**, *7*, 89–99.
- (32) Lemaire, H. P.; Livingston, R. L. *J. Am. Chem. Soc.* **1952**, *74*, 5732–6.
- (33) Miller, F. A.; Capwell, R. J. *Spectrochim. Acta, Part A* **1971**, *A 27*, 1113–31.
- (34) ElSohly, A. M.; Tschumper, G. S.; Crocombe, R. A.; Wang, J. T.; Williams, F. *J. Am. Chem. Soc.* **2005**, *127*, 10573–83.
- (35) Gallup, G. A. *Chem. Phys. Lett.* **2004**, *399*, 206–9.
- (36) Johnson, M. A.; Lineberger, W. C. Pulsed Methods for Cluster Ion Spectroscopy. In *Techniques for the Study of Ion-Molecule Reactions*; Farrar, J. M., Saunders, W. H., Eds.; Wiley: New York, 1988; Vol. 20; pp 591–635.
- (37) Robertson, W. H.; Kelley, J. A.; Johnson, M. A. *Rev. Sci. Instrum.* **2000**, *71*, 4431–4.
- (38) Posey, L. A.; Deluca, M. J.; Johnson, M. A. *Chem. Phys. Lett.* **1986**, *131*, 170–4.
- (39) Okumura, M.; Yeh, L. I.; Myers, J. D.; Lee, Y. T. *J. Chem. Phys.* **1986**, *85*, 2328–9.
- (40) Burnett, S. M.; Stevens, A. E.; Feigerle, C. S.; Lineberger, W. C. *Chem. Phys. Lett.* **1983**, *100*, 124–8.
- (41) Leopold, D. G.; Murray, K. K.; Miller, A. E. S.; Lineberger, W. C. *J. Chem. Phys.* **1985**, *83*, 4849–65.
- (42) Wenthold, P. G.; Polak, M. L.; Lineberger, W. C. *J. Phys. Chem.* **1996**, *100*, 6920–6.
- (43) Grimsrud, E. P.; Chowdhury, S.; Kebarle, P. *J. Chem. Phys.* **1985**, *83*, 1059–68.
- (44) Nielsen, S. B.; Ayotte, P.; Kelley, J. A.; Johnson, M. A. *J. Chem. Phys.* **1999**, *111*, 9593–9.
- (45) Corcelli, S. A.; Kelley, J. A.; Tully, J. C.; Johnson, M. A. *J. Phys. Chem. A* **2002**, *106*, 4872–9.
- (46) McDowell, R. S.; Krohn, B. J. *Spectrochim. Acta, Part A* **1986**, *42*, 371–85.
- (47) Brinkmann, N. R.; Schaefer, H. F. *Chem. Phys. Lett.* **2003**, *381*, 123–8.
- (48) Morokuma, K. Personal communication.
- (49) Johnson, M. A.; Rostas, J.; Zare, R. N. *Chem. Phys. Lett.* **1982**, *92*, 225–31.
- (50) Johnson, M. A.; Alexander, M. L.; Hertel, I.; Lineberger, W. C. *Chem. Phys. Lett.* **1984**, *105*, 374–9.
- (51) Mead, R. D.; Hefter, U.; Schulz, P. A.; Lineberger, W. C. *J. Chem. Phys.* **1985**, *82*, 1723–31.
- (52) Ervin, K. M.; Ho, J.; Lineberger, W. C. *J. Chem. Phys.* **1989**, *91*, 5974–92.
- (53) Ervin, K. M.; Lineberger, W. C. *J. Phys. Chem.* **1991**, *95*, 1167–77.
- (54) Kim, J. B.; Wenthold, P. G.; Lineberger, W. C. *J. Chem. Phys.* **1998**, *108*, 830–7.
- (55) Lineberger, W. C.; Woodward, B. W. *Phys. Rev. Lett.* **1970**, *25*, 424–8.
- (56) Hiraoka, K.; Mizuno, T.; Eguchi, D.; Takao, K.; Iino, T.; Yamabe, S. *J. Chem. Phys.* **2002**, *116*, 7574–82.